Journal of Hydrology 617 (2023) 129097

Contents lists available at ScienceDirect

Journal of Hydrology

journal homepage: www.elsevier.com/locate/jhydrol

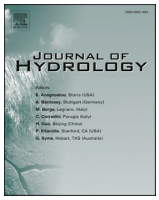

On the application of rainfall projections from a convection-permitting climate model to lumped catchment models

M.J. Ascott [a,*], V. Christelis [b], D.J. Lapworth [a], D.M.J. Macdonald [a], C. Tindimugaya [c], A. Iragena [c], D. Finney [d], R. Fitzpatrick [d], J.H. Marsham [d], D.P. Rowell [e]

[a] British Geological Survey, Maclean Building, Benson Lane, Crowmarsh Gifford, Oxfordshire OX10 8BB, UK
[b] British Geological Survey, Nicker Hill, Keyworth, Nottinghamshire NG12 5GG, UK
[c] Directorate of Water Resources Management, Ugandan Ministry of Water and Environment, Plot 17 Mpigi Road, Entebbe, Uganda
[d] School of Earth and Environment, University of Leeds, and National Centre for Atmospheric Science, Leeds, UK
[e] Met Office Hadley Centre, Exeter, UK

ARTICLE INFO

Keywords:
Climate change
River flows
Convection-permitting model
Lake Victoria

ABSTRACT

Climate change is predicted to increase rainfall intensity in tropical regions. Convection permitting (CP) climate models have been developed to address deficiencies in conventional climate models that use parameterised convection. However, to date, precipitation projections from CP climate models have not been used in conjunction with hydrological models to explore potential impacts of explicit modelling of convective rainfall on river flows in the tropics. Here we apply the outputs of a continental scale CP climate model as inputs to lumped rainfall-runoff models in Africa for the first time. Applied to five catchments in the Lake Victoria Basin, we show that the CP climate model produces greater river flows than an equivalent model using parameterised convection in both the current and future (c. 2100) climate. However, the location of the catchments near to Lake Victoria results in limited changes in extreme rainfall and river flows relative to changes in mean rainfall and river flows. Application of CP model rainfall data from an area where rainfall extremes change more than the change in mean rainfall to the rainfall-runoff model does not result in significant changes in river flows. Instead, this is shown to be a result of the rainfall-runoff model structure and parameterisation, which we posit is due to large-scale storage in the catchments associated with wetland cover, that buffers the impact of rainfall extremes. Based on an assessment of hydrological attributes (wetland coverage, water table depth, topography, precipitation, evapotranspiration and river flow) using global-scale datasets for the catchments in this research, this buffering may be extensive across humid regions. Application of CP climate model data to lumped catchment models in these areas are unlikely to result in significant increases in extreme river flows relative to increases in mean flows.

1. Introduction

Climate change is predicted to result in increasing rainfall intensity in sub-Saharan Africa (Dunning et al., 2018), with these increases predicted to affect water resources (Cuthbert et al., 2019; Ngoran et al., 2015; Taylor et al., 2013). The impacts of climate change on water resources have been assessed extensively globally (see reviews by Ataw-neh et al. (2021); Garrote (2017)) including in sub-Saharan Africa (Kusangaya et al., 2014; Ngoran et al., 2015). Conventional approaches (Fowler et al., 2007) to the assessment of the impacts of climate change on water resources consist of the use of downscaled meteorological data from coarse scale (horizontal resolution > 100 km) global circulation models (GCMs, e.g CMIP5 (Taylor et al., 2012)) under current and future climate to hydrological models. These approaches are limited by the extent to which GCMs can reliably simulate the climate physics of an area of interest. In tropical continental regions such as sub-Saharan Africa, GCMs are known to exhibit large errors in precipitation associated with the representation of convective rainfall (Bock et al., 2011). GCMs parameterise convective rainfall resulting in too much light daily rainfall and too little intense rainfall (Dirmeyer et al., 2012; Stephens et al., 2010), which is a significant deficiency in tropical areas where convective systems can be c. 75 % of total rainfall (Roca et al., 2014).

* Corresponding author.
E-mail address: matta@bgs.ac.uk (M.J. Ascott).

https://doi.org/10.1016/j.jhydrol.2023.129097

Available online 7 January 2023

In order to address the deficiency of parameterised convection in GCMs, "convection-permitting" climate models (CPMs) have been developed. These models are run at kilometre-scale grid resolution, with convection represented explicitly on the model grid (Kendon et al., 2021). CPMs have been shown to produce significant improvements in model performance in comparison to conventional parameterised models in both small scale rainfall characteristics (e.g. intensity, diurnal cycles) and large-scale circulation in Africa (Senior et al., 2021), with improvements also observed in Europe (Berthou et al., 2020) and the USA (Liu et al., 2017). The use of convection permitting models in operational rainfall forecasting is now well established (Clark et al., 2016). Rainfall forecasts have also been translated into forecasts of flash flooding in the UK (Golding et al., 2016), Mediterranean (Vincendon et al., 2011) and USA (Qing et al., 2020; Wang and Wang, 2019; Zhang et al., 2021). Recently, convection permitting models have been used to explore the impacts of climate change on short duration extremes in precipitation, with continental scale CP projections in Africa producing greater future increases in 3 h and daily precipitation than parameterised models (Kendon et al., 2017; Kendon et al., 2019). This is due at least in part to greater intensification of the storm updrafts, which are not explicitly modelled in standard, parameterised models (Jackson et al., 2020). As convection-permitting models give greater intensification of extreme rainfall under climate change through better capturing the dynamics of storms and their couplings with larger scales, we therefore expect use of convection-permitting model projections of rainfall to affect projections of hydrological flows. The impacts of climate change based on CP projections on river flows based on distributed hydrological models have been evaluated in temperate climates such as the UK and northern and alpine Europe (Kay, 2022; Kay and Davies, 2008; Reszler et al., 2018; Schaller et al., 2020) and semiarid Texas (Wang and Wang, 2019). Recently Miller et al. (2022) used CP projections to develop design storms to feed into an urban flood model in Burkina Faso, West Africa. To date, however, no research has assessed how future changes in precipitation produced by convection-permitting models may affect projected river flows derived from lumped hydrological models in the tropics. Moreover, globally no work has assessed how lumped conceptual hydrological model structure and parameterisation may affect the propagation of extreme events from CPM precipitation to hydrological model river flow.

In this paper, we quantify changes in river flows associated with application of convection-permitting climate model data to lumped conceptual hydrological models for the first time. We apply precipitation data from a high-resolution convection-permitting climate model for Africa to five lumped conceptual hydrological models across the Lake Victoria Basin, East Africa, and compare the resulting river flow projections with projections derived from application of an equivalent climate model with parameterised convection. We also undertake a series of model experiments applying climate model precipitation data from a region of known modelled rainfall intensification to each of the hydrological models and explore how changes in rainfall intensity propagate through the hydrological models. Finally, we consider the implications for use of convection-permitting climate model data in hydrological modelling studies and water management.

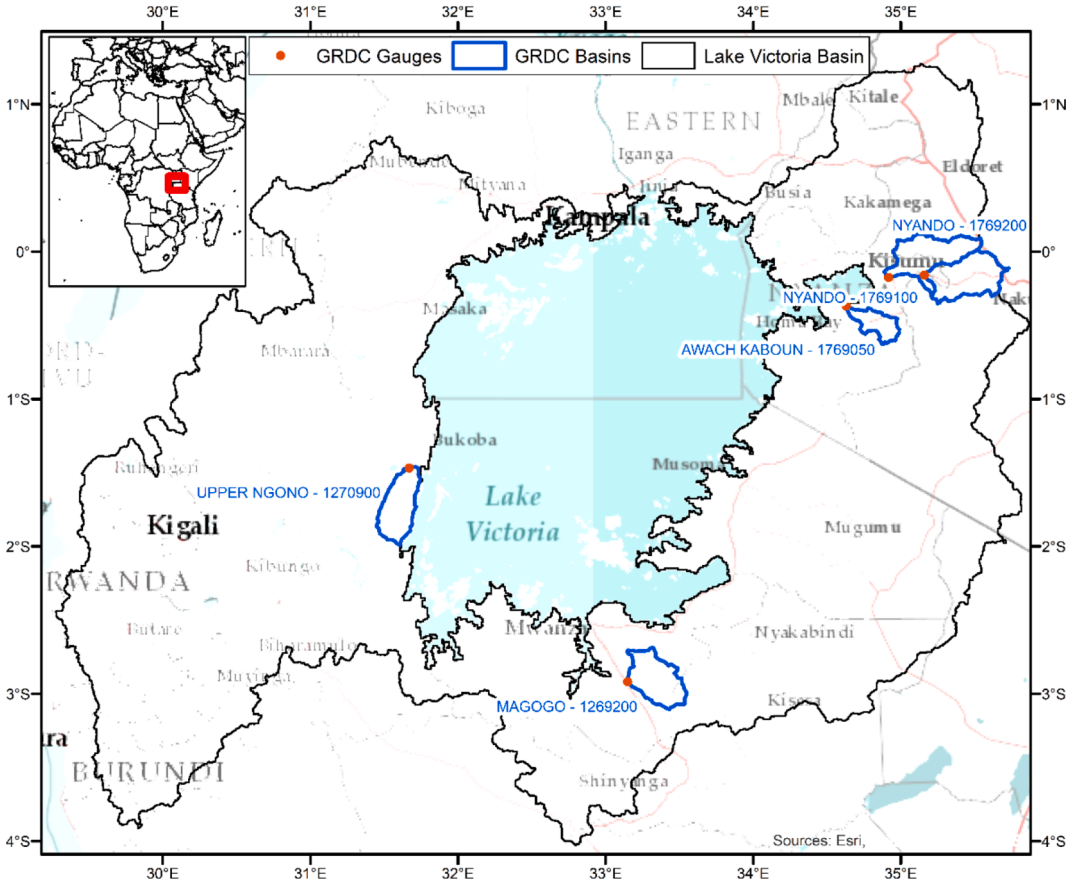

Fig. 1. Lake Victoria Basin (black), East Africa, and the location of Global Runoff Data Centre (GRDC) catchments (blue) and gauges (red), reproduced with permission of GRDC (2011)). Lake Victoria in light blue. Lake Victoria Basin reproduced after Lehner et al. (2008) and Lehner and Grill (2013). The inset map shows the location of the study area (red) in the African continent. (For interpretation of the references to colour in this figure legend, the reader is referred to the web version of this article.)

2. Materials and methods

2.1. Study area and hydroclimatic context

The study area for this research is the Lake Victoria Basin (LVB), East Africa (Fig. 1). The LVB is located at the head of the Nile River Basin and has a total area of c. 251,000 km^2. The area has an equatorial climate with a bimodal rainfall pattern ("long rains" from March to May, and "short rains" from October to December). Numerous studies have evaluated impacts of climate change on river flows using lumped and semi-distributed models in the LVB (Dessu and Melesse, 2013; Gabiri et al., 2020; Githui et al., 2009; Kingston and Taylor, 2010; Mehdi et al., 2021; Taye et al., 2011) and the wider East African region (Meresa and Gatachew, 2018; Siam and Eltahir, 2017; van Griensven et al., 2012). However, previous studies used downscaled GCM outputs which parameterize convection. None have evaluated the impact of explicit modelling of convective processes on river flow projections. The LVB is a hotspot for severe convective storms (Hanley et al., 2021), and floods and landslides associated with such extreme weather events (e.g. the 2019 short rains (Wainwright et al., 2021a)) have significant socioeconomic consequences. There is large inter-model uncertainty in the region (Bornemann et al., 2019) and GCMs are known to have significant biases to convective rainfall, with both CMIP5 and CMIP6 models shown to poorly simulate extreme events (Ayugi et al., 2021) in East Africa. Consequently, some workers have developed CPM runs of the regional historic climate (Hanley et al., 2021; Van de Walle et al., 2020) for the purposes of improved understanding of regional climate and forecasting. At climate change timescales, CPM runs have been developed at the continental scale in Africa (Kendon et al. (2019); Stratton et al. (2018), and used in this research). These have been evaluated in East Africa (and the LVB in particular) and have been shown to improve simulations of rainfall intensity and the diurnal cycle (Finney et al., 2019; Finney et al., 2020).

2.2. Hydrological model development

2.2.1. Model code

The hydrological model used in this research was the lumped conceptual hydrological model GR4J (Perrin et al., 2003). GR4J has been used extensively for streamflow simulation worldwide and has been shown to perform, on average, well over a wide range of catchment conditions whilst remaining parsimonious (Perrin et al., 2003; Westra et al., 2014). GR4J has also been used in sub-Saharan Africa in particular (Bodian et al., 2018; Kodja et al., 2020; Le Lay et al., 2007). The structure of GR4J is shown in Fig. 2. The model runs on a daily timestep is driven by single time series of precipitation (P) and potential evapotranspiration (E). The model consists of two stores ("production" and "routing") and four parameters (x_1–x_4). Net rainfall (P_n), actual evapotranspiration (E_s) and net evapotranspiration (E_n) are calculated from the balance on P and E. A fraction of P_n, P_s, then is transferred to the production store, which has a maximum capacity x_1 and level S. Percolation out of the production store, PERC, is added to P_n-P_s to form the water quantity reaching the routing part of the model, P_r. The routing store algorithms divide P_r into direct and indirect flow components using unit hydrograph approaches (UH1 and UH2, with the time base as parameter x_4) to spread effective rainfall over several successive timesteps to produce hydrograms Q9 and Q1. Both the direct and indirect flow components via the routing store (maximum capacity parameter x_3, level R) account for groundwater exchange using parameter x_2, and resulting flow components (Q_r and Q_d) are combined to produce the total streamflow Q. For more information regarding the model structure of GR4J, the reader is referred to Perrin et al. (2003).

2.2.2. River flow observations, driving data and model calibration

In order to test the impact of convection-permitting climate model data on river flows, GR4J was run on a daily timestep. In order to calibrate GR4J's current climate, we therefore extracted all daily river flow data in the Global Runoff Data Centre (GRDC, 56,068 Koblenz, Germany) for a bounding box covering the LVB (28-37°E, 5°S – 4°N). This consisted of daily river flow data for five catchments in the LVB, as shown in Fig. 1. A summary of metadata for each of the catchments is

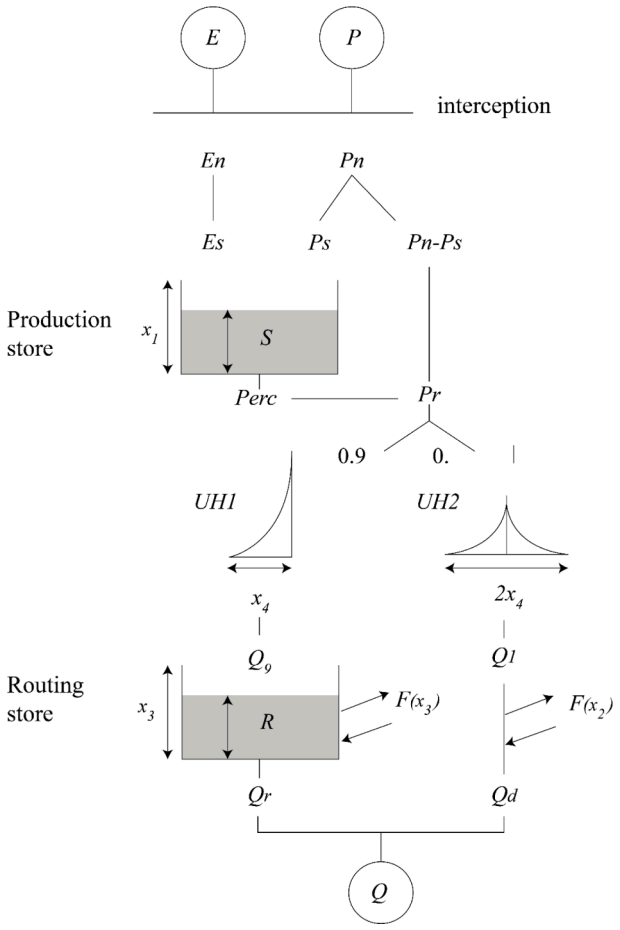

Fig. 2. Structure of GR4J. Reproduced after Perrin et al. (2003) with permission from Elsevier. Meaning of acronyms are included in the text.

Table 1
Summary of metadata for each of the catchments used in this research.

Catchment ID	River name	Country	Catchment size (km^2)	Number of data points	Start/ end dates
1269200	MAGOGO	Tanzania	1187	730	1978-01-01: 1979-12-31
1270900	UPPER NGONO	Tanzania	1161	730	1978-01-01: 1979-12-31
1769050	AWACH KABOUN	Kenya	540	1096	1978-01-01: 1980-12-31
1769100	NYANDO	Kenya	2625	1096	1978-01-01: 1980-12-31
1769200	NYANDO	Kenya	1419	1065	1978-02-01: 1980-12-31

shown in Table 1.

For each of the five catchments we developed a GR4J model instance by adjusting its parameters using the R Package AirGR (Coron et al., 2017) (referred to as "each GR4J model" herein). Each GR4J model requires single time series of precipitation and potential evapotranspiration (PET) as driving datasets. We extracted historical (1958–2001) daily rainfall time series from the WATCH forcing dataset (Weedon et al., 2011), taking the spatial mean of all grid cells within each catchment. We also extracted temperature data which was used to calculate PET using the Thornthwaite (1948) method. Each GR4J model was calibrated using the full river flow time series, which has been shown to be more robust than calibration and validation using a split-sample approach (Arsenault et al., 2018). The model was calibrated using the default range of parameters and the built in steepest descent local slope procedure (Coron et al., 2017) to optimise the Kling-Gupta Efficiency (KGE) (Gupta et al., 2009). The KGE is a calculated as:

$$KGE = 1 - \sqrt{(r-1)^2 + \left(\frac{\sigma_{sim}}{\sigma_{obs}} - 1\right)^2 + \left(\frac{\mu_{sim}}{\mu_{obs}} - 1\right)^2}$$

Where r is the linear correlation between observations and simulations, σ_{sim} and σ_{obs} are the standard deviations in the simulations and observations respectively, and μ_{sim} and μ_{obs} are the means of the simulations and observations respectively. The KGE has an "ideal" value at unity. It should be noted that for our application the use of population-based optimization algorithms which presumably have better global search capabilities did not outperform the default local approach in GR4J. The KGE was chosen instead of other criteria, such as the Nash-Sutcliffe Efficiency, as this research focusses on changes in extreme rainfall and river flows. In such cases, the KGE tends to constrain the underestimation of uncommon flow events in simulated runoff (Gupta et al., 2009).

2.3. Application of climate model experimental data to hydrological models

For each of the calibrated GR4J models, we applied data from two climate model experiments (Stratton et al., 2018) developed with the specific aim of evaluating the impact of explicit modelling of convection: (1) "R25", a 25 km resolution climate model over Africa with parameterised convection and (2) "CP4", a finer 4 km resolution climate model over Africa which allows structures recognizable as convective clouds to form. The two climate models provide 10 year time series of daily rainfall and temperature for a historic (1997–2007) and future (c. 2100) period (Finney et al., 2020; Kendon et al., 2019). CP4 is the first convection-permitting multiyear regional climate simulation on an Africa-wide domain (Senior et al., 2021). The 25 km resolution of R25 reflects the global 25 km AMIP simulation used as a boundary condition for both CP4 and R25. The 4 km resolution for CP4 was used as a compromise between domain size (the African continent), computational cost and the ability of the model to resolve deep convection (Stratton et al., 2018). The length of time series produced by CP4 and R25 was a balance between computational demands and the need to generate sufficient data to evaluate the impact of resolving convection. Full information on the CP4 and R25 model experimental design can be found in Stratton et al. (2018). A number of previous papers are available which evaluate CP4 and R25 model results (Finney et al., 2019; Finney et al., 2020; Kendon et al., 2019; Senior et al., 2021) and use these results for rainfall downscaling (Wilby et al., 2022).

To directly test the impact of explicit modelling of convective precipitation on predicted river flows, we made the deliberate decision not to bias-correct or downscale the CP4 and R25 data. Use and evaluation of CP4 and R25 data in this manner has an additional benefit of informing decisions on the value of bias correction of CPM data and the level of sophistication used in future studies. Notwithstanding that the purpose of this paper is to assess the impact of explicit modelling of convective precipitation, it should be noted that previous studies have evaluated CP4 and R25 against observations and these have shown that both simulations capture many broad features of precipitation across east Africa. These include the biannual progression of the tropic rainband, the contrasting rainfall between the African Rift and the Horn of Africa (Finney et al., 2019), the interannual variability in the peak of the short rains and the balance of precipitation between long and short rains (Wainwright et al., 2021b). The 4 km CP4 outputs were regridded using area-weighted, bi-linear interpolation to 25 km. Regridding CP4 allows for a comparison with R25 on the basis of explicit and parametrised convection, opposed to differences in resolution. The results presented are representative of rainfall statistics on the scale of the R25 model (Finney et al., 2019). Spatial mean daily time series for each catchment in Fig. 1 were extracted and applied to each GR4J model.

Projected changes in both mean and extreme precipitation from CP4 have been shown to be spatially variable both at the continental scale (Kendon et al., 2019) and also in East Africa in particular (Finney et al., 2020). To evaluate how changes in precipitation propagate through each of the GR4J models developed in this research, we conducted a sensitivity experiment by applying the same set of CP4 driving data to each GR4J model. CP4 precipitation and temperature data was used from an area of known precipitation intensification to each of the GR4J models. For each 25 km grid cell, we first calculated the ratio of the changes in daily extreme precipitation (defined as the 95th percentile of all days) to changes in daily mean precipitation between the historic and future CP4 runs, as follows:

$$\Delta 95/\Delta mean = \frac{95_{future}/95_{historic}}{mean_{future}/mean_{historic}}$$

The resulting ratio (referred to as Δ95/Δmean herein) is shown in Fig. 3. The spatial distribution of the Δ95/Δmean metric explicitly shows how modelled precipitation may intensify over a region. Where Δ95/Δmean > 1, the change in the extreme (as defined by the 95th percentile) is greater than the change in the mean. Where Δ95/Δmean < 1, the change in the mean is greater than the change in the extreme. The 95th percentile was used as this has been used extensively in the analysis of extremes in precipitation (Christensen and Christensen, 2003) in additional to inland fluvial (Wu et al., 2012), groundwater (Ascott et al., 2017) and coastal flooding (Pirazzoli et al., 2006). We selected a bounding box (34.37–34.90 °W, 0.82–1.36 °S, blue dashed line in Fig. 3) where Δ95/Δmean > 1 and extracted and applied the

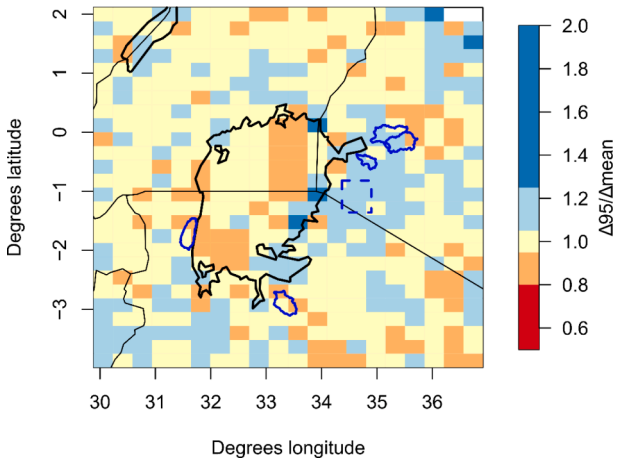

Fig. 3. Δ95/Δmean (unitless) for CP4 precipitation across the LVB region. Blue colours indicate where Δ95/Δmean is > 1 (i.e. the change in the extreme (as indicated by the 95th percentile) is greater than the change in the mean). Red colours indicate where Δ95/Δmean is < 1 (i.e. the change in the mean is greater than the change in the extreme). Catchments are shown by the solid blue lines and the area of intensifying rainfall used in the hydrological model experiments is shown by the dashed blue line. Thin and thick black lines are country and lake (principally Lake Victoria) boundaries respectively.

precipitation and temperature data to each of the hydrological models.

2.4. Analysis of model results

We first evaluated the calibrated historic river flow through visual inspection of the time series and KGE values. We then evaluated the river flow projections generated by the application of the catchment-specific meteorological data from CP4 and R25. This was first done visually through plotting of river flow quantiles and boxplots for each hydrological model. We then calculated if there are statistically significant differences between modelled river flows produced by GR4J using data from: (1) CP4-Future and CP4-Historical, (2) R25-Future and R25-Historical, (3) CP4-Future and R25-Future, (4) CP4-Historical and R25-Historical. For each of these comparisons we undertook a two-sample *t* test (Webster and Oliver, 1990) and a two-sample Kolmogorov-Smirnov test (Conover, 1999) to determine if there were significant differences in the mean and distribution of river flows respectively. We then calculated Δ95/Δmean for each model for precipitation and river flow. For the GR4J model experiment runs, we calculated and plotted river flow quantiles and boxplots and then calculated Δ95/Δmean for precipitation, river flow and the hydrological model intermediate terms PERC, Q9 and Q_r (Fig. 2). All analysis was conducted using the statistical computing environment R (R Development Core Team, 2016).

3. Results

3.1. Hydrological model calibration

Fig. 4 shows the observed and modelled historic river flows produced by GR4J for each of the catchments in this research. The calibrated model parameter sets and resulting KGE values are reported in Table 2. Across the five catchments, observational data for daily river flows are

Table 2
Calibrated model parameters (x_1–x_4, see Fig. 2) for each catchment and Kling-Gupta Efficiency (KGE).

Catchment ID	x_1	x_2	x_3	x_4	KGE
1269200	60.62	−30.41	146.83	2.30	0.60
1270900	295.89	1.66	615.56	20.00	0.81
1769050	114.56	−29.96	667.54	2.38	0.43
1769100	411.43	−36.84	215.97	1.16	0.46
1769200	64.31	−45.03	335.67	2.40	0.45

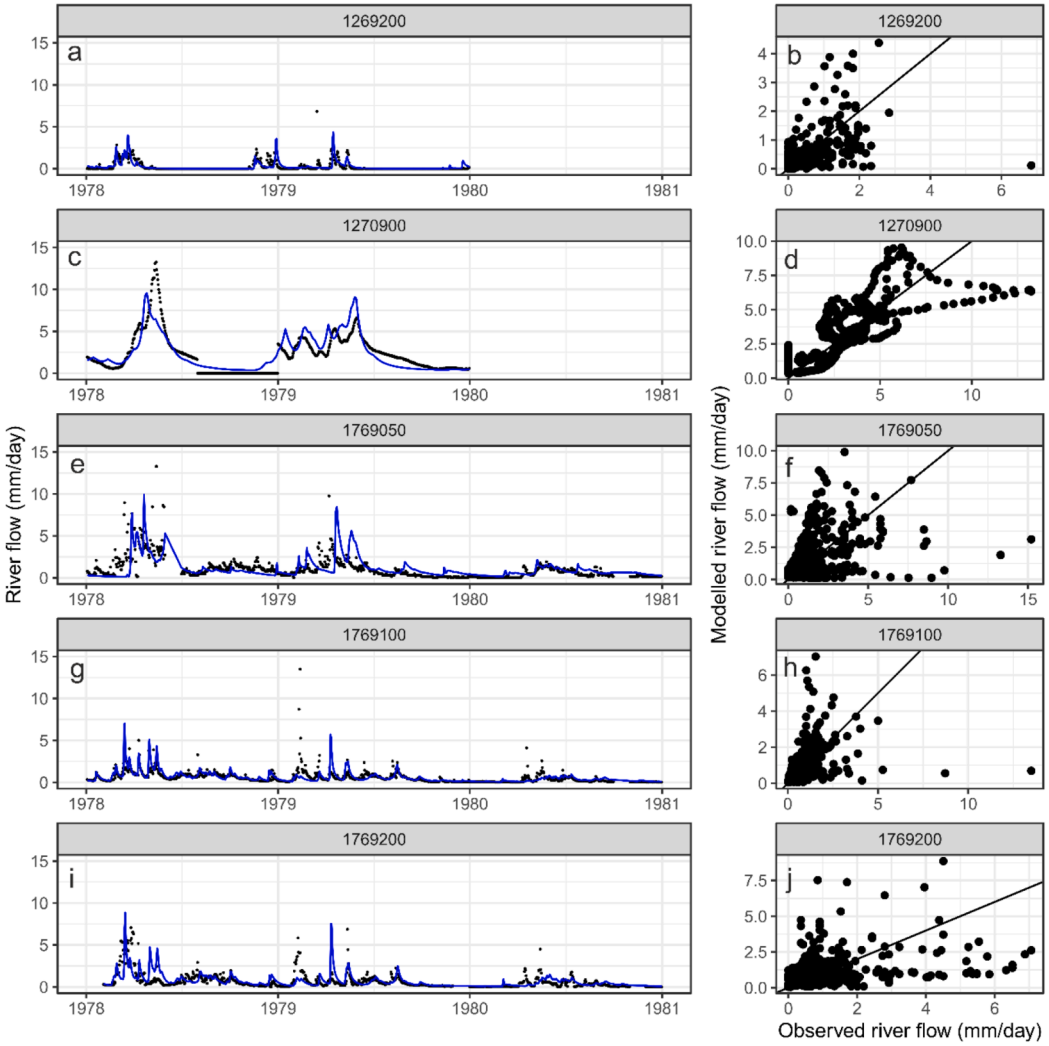

Fig. 4. Observed and modelled river flows for the five catchments used in this research. Data are presented as time series (left, observed in black dots and modelled in blue lines) and scatterplots (right, black line is the 1:1 line, text in grey boxes are catchment IDs corresponding to Fig. 1 and Table 1). Observed data provided by The Global Runoff Data Centre, 56,068 Koblenz, Germany. (For interpretation of the references to colour in this figure legend, the reader is referred to the web version of this article.)

sparse, with data only available in the 1970s-1980s. The implications of this are discussed further in section 4.3. When driven using historical WATCH forcing data, the GR4J catchment models appear to replicate the timing and magnitude of the observed river flow peaks and recessions reasonably well (Fig. 4). At low to moderate river flows (0–5 mm/day) the GR4J catchment models appear neither systematically over nor underpredicting river flows, whilst at higher river flows (5 – 15 mm/day) the models appear to slightly underestimate peak flows. Using the mean observed flow as a benchmark, the KGE values for each model are moderately good (Table 2), and within the range of values ($-0.41 < KGE \leq 1$) that could be considered "reasonable" (Knoben et al., 2019).

3.2. *River flow projections for each catchment derived from application of CP4 and R25 data*

Fig. 5 shows river flow quantiles produced by GR4J for each of the catchments when applying the historic and future CP4 and R25 data. The same results are presented as boxplots in Figure S2. It can be observed that across the river flow quantiles, application of the future model runs of CP4 and R25 to GR4J produces greater river flows than the historic model runs. With the exception of catchment 1269200 (Fig. 5 panel a), application of CP4 data also produces greater river flows than application of R25 to GR4J (Fig. 5). In catchment 1269200 R25-

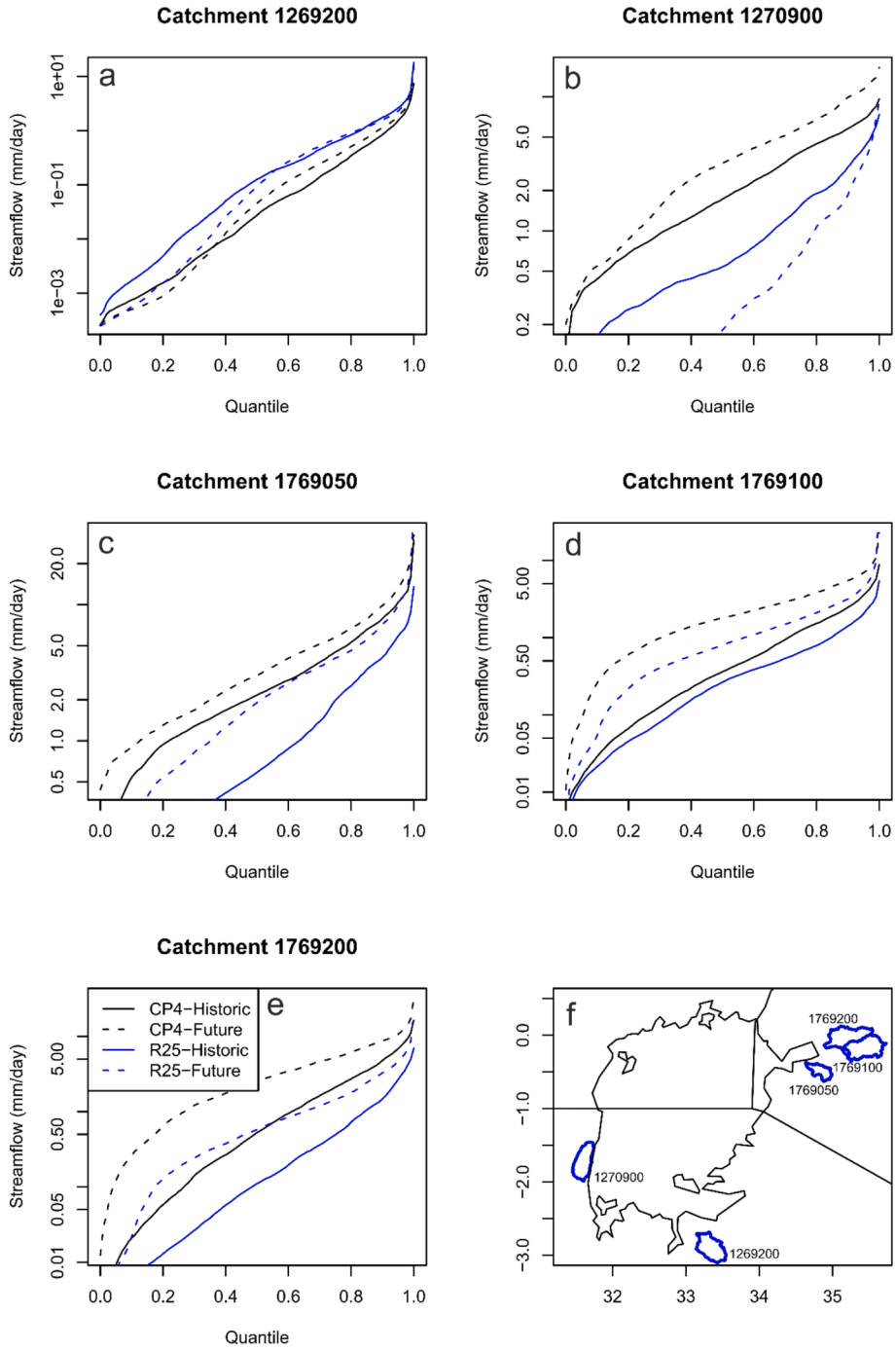

Fig. 5. River flow quantiles (y-axis log scale) for each catchment for historic and future CP4 and R25 model runs. Panel f shows the locations of the catchments (blue lines) in the context of Lake Victoria and country boundaries (black lines). Catchment IDs correspond to those shown in Fig. 1 and Table 1. (For interpretation of the references to colour in this figure legend, the reader is referred to the web version of this article.)

Table 3
Modelled changes in extreme precipitation (P) and river flow (Q) relative to the mean (Δ95/Δmean) for CP4 and R25 for the five catchments used in this research.

	CP4		R25	
Catchment ID	P	Q	P	Q
1269200	0.96	0.89	0.96	0.90
1270900	0.99	1.02	1.00	1.31
1769050	1.05	0.95	0.99	0.79
1769100	0.97	0.71	1.01	0.81
1769200	0.92	0.68	0.96	0.75

Historic produces greater river flows than R25-Future and CP4 runs for quantiles 0–0.5, before the R25 runs begin to converge between quantiles 0.5 and 1. The R25-Future run in catchment 1270900 (Fig. 5 panel b) produced zero flow for quantiles 0–0.5.

For all catchments there were significant ($p < 0.01$) differences in the mean (based on two sample *t*-test) and distribution (based on two sample Kolmogorov-Smirnov test) of river flows between runs driven by (1) CP4-Future and CP4-Historical, (2) R25-Future and R25-Historical, (3) CP4-Future and R25-Future, (4) CP4-Historical and R25-Historical.

Table 3 shows Δ95/Δmean for CP4 and R25 for each of the five catchments. With the exception of catchment 1270900, for all other catchments and both CP4 and R25, Δ95/Δmean is greater for precipitation than for river flow.

3.3. GR4J model experiment results

Fig. 6 shows river flow quantiles when CP4 data for the box where rainfall intensifies (Fig. 3) is applied to each of the GR4J models (see also Figure S3). It can be observed that application of CP4 data to GR4J results in greater river flows than R25. Table 4 shows Δ95/Δmean for precipitation, river flow and model intermediate terms for each of the GR4J models. Δ95/Δmean is greater for P, PERC and Q9 than for Q_r and Q.

4. Discussion

4.1. Impacts of convection permitting climate model runs on river flows and the role of lumped hydrological model structure

When applying data from the climate model experiments to each lumped catchment model, the future runs result in greater river flows than the historic runs (Fig. 5), with significantly different ($p < 0.01$) river flow means and distributions. Apart from one catchment (1269200), application of CP4 data resulted in greater river flows than application of R25 data (see Fig. 5 panel a). For all catchments application of CP4 data resulted in significantly different ($p < 0.01$) river flow means and distributions in comparison to application of R25. We suggest that the differences between the catchments in modelled river flows are likely primarily due to small-scale chaotic variability in sampling of convective precipitation events around the LVB, more than physical differences in surface forcing, such as topography and land use, lakeside features (Rowell and Berthou, 2022). Longer, or ensemble, climate simulations would better discriminate the impact of heterogeneous surface features. For CP4, with the exception of low flows (<quantile 0.4) at catchment 1269200, projected increases in river flows occur across all quantiles for all catchments (Fig. 5, Figure S1 in Supplementary Material), reflecting an increase in mean precipitation, but with limited increases in extreme flows relative to changes in mean flows, despite the similarity of increases in mean and extreme precipitation (Table 3). When applying CP4 data from an area where increases in extreme precipitation are greater than increases in the mean, the same also occurs (Table 4). Why are increases in extreme precipitation relative to increases in the mean precipitation not propagating to changes in river flows? The changes in Δ95/Δmean in different terms of GR4J (Table 4) suggest this is the result of the hydrological model structure used in this research. Δ95/Δmean decreases substantially between the terms Q9 and Q_r (Table 4), which is associated with the routing store and groundwater exchange components of the model (Fig. 2). We posit that the storage dynamics in the routing store (Fig. 2) result in a dampening of extreme precipitation events. Moreover, in four out of five of the calibrated catchment models developed in this research, the groundwater exchange parameter is negative (Table 2), which results in the model losing excess water during extreme precipitation events. These storage dynamics are common across many lumped hydrological modelling approaches (e.g. HBV (Bergström, 1995), HEC-HMS (Gyawali and Watkins, 2013), NAM (DHI, 2008)) and thus similar results would be anticipated if the CP4 and R25 precipitation data were applied to such models.

What physical processes are likely to be leading the dampening of extreme precipitation events in reality? Whilst the structure and parameter sets of lumped conceptual models such as GR4J have limited physical basis (Perrin et al., 2003), some insight can be gained from the attributes of the catchments used in this research. The catchments are reported to have notable wetland coverage (mean 30% of land use), shallow water tables (mean depth 1.5 m below ground level) and surface topography (mean slope 2.82°), with annual precipitation (mean 1400 mm) and AET (mean 1130 mm) being much greater than river flow (mean 314 mm) (Linke et al., 2019). It is therefore likely that at the catchment scale, storage and evaporative losses from wetlands and shallow groundwater storage will dampen the impacts of increases in extreme precipitation on catchment outflows. Such catchment attributes are likely to be globally common. Fig. 7 shows the global distribution of shallow water tables (panel a), wetlands (panel b), and where runoff is <25 % of precipitation (panel c). There are large areas of the Americas, Europe, Asia and Africa where shallow water tables and wetland coverage may result in dampening of extreme precipitation events at the catchment scale.

4.2. Implications for water management

The changes in rainfall and river flow distribution predicted by application of CP4 and R25 data have significant implications for both water resources and flood risk management under future climate change. Whilst no significant increases in extremes relative to increases in mean river flows were projected for these LVB catchments, application of CP4 still resulted in greater predicted river flows than application of R25 in the future model runs in four out of five catchments. Such sensitivities – likely location-specific – should be borne in mind when evaluating the impacts of climate change on river flows by applying the output of conventional climate models which parameterise convection (e.g. CMIP5 (Taylor et al., 2012)).

Increases in extreme precipitation relative to increases in mean precipitation shown in CP4 (blue in Fig. 3) is likely to affect projections of future flooding. It is anticipated that Δ95/Δmean associated with CP4 precipitation would propagate more extensively though a high temporal and spatial resolution flood inundation model (e.g. Yu and Lane (2006)) due to the distributed nature of such modelling approaches.

4.3. Limitations and further work

There are a number of limitations to this research which could be addressed by further work. These are outlined below. The observed river flow time series used in the model calibration are short and from the 1970s and 1980s. These are the only publicly available daily river flow data in the Lake Victoria Basin, and this paucity of observational data is present across much of Africa (Tramblay et al., 2021). Similarly, we used a reanalysis based set of driving data to calibrate the hydrological models (Weedon et al., 2011), which may have contributed to the underestimation of peak flows by the calibrated GR4J catchment models. In addition to new river flow and precipitation observations, further

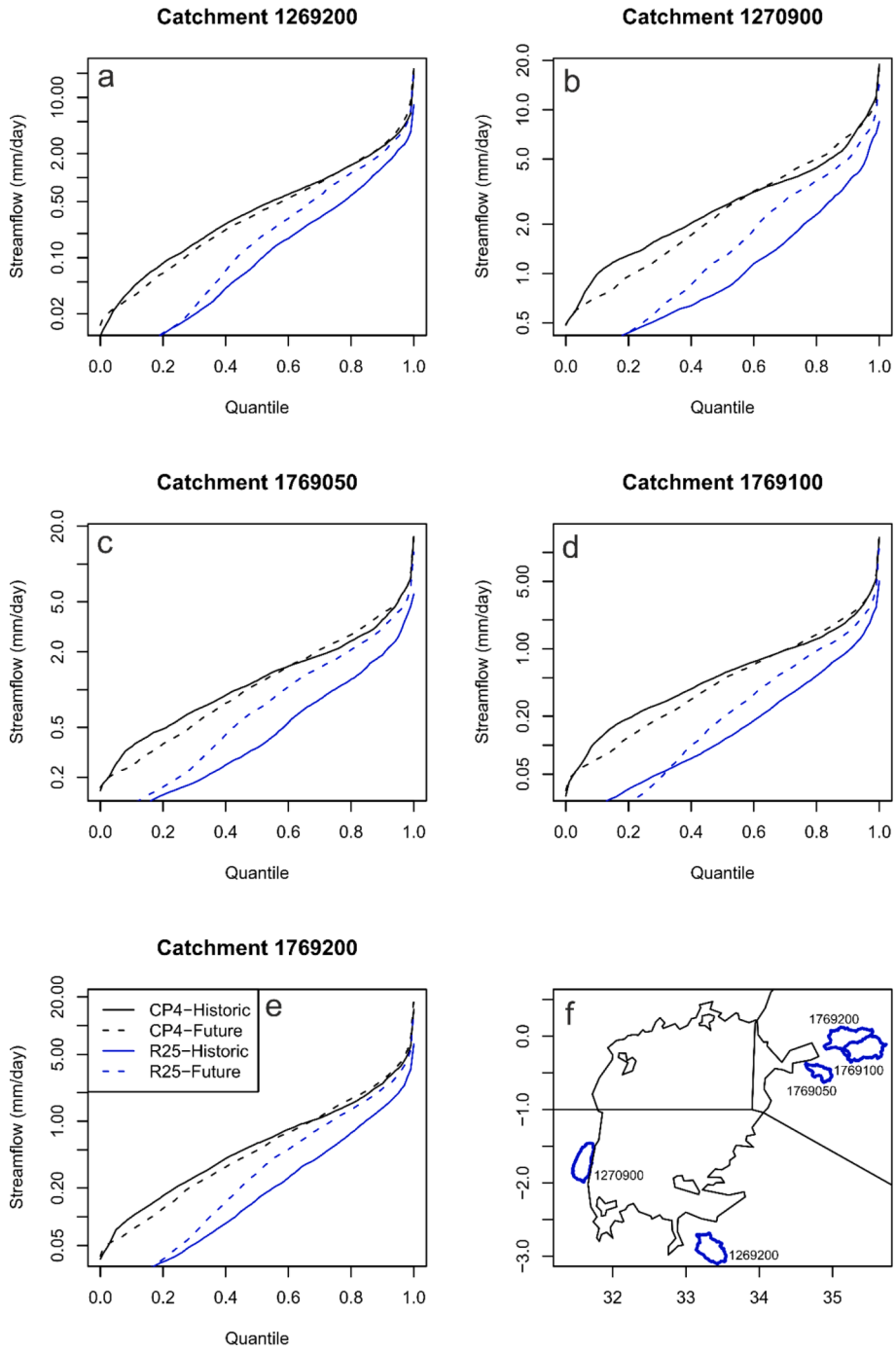

Fig. 6. River flow quantiles (y-axis log scale) for catchment models driven by CP4 data for the box shown in Fig. 3. Panel f shows the locations of the catchments (blue lines) in the context of Lake Victoria and country boundaries (black lines). Catchment IDs correspond to those shown in Fig. 1 and Table 1. (For interpretation of the references to colour in this figure legend, the reader is referred to the web version of this article.)

Table 4
Modelled changes in extreme precipitation (P), model terms (see Fig. 2) PERC, Q9, Q_r, and river flow (Q) relative to the mean (Δ95/Δmean) for the catchment model driven by CP4 data for the box in Fig. 3.

Catchment ID	P	PERC	Q9	Q_r	Q
1269200	1.09	1.27	1.10	1.06	1.06
1270900	1.09	1.13	1.08	0.98	0.99
1769050	1.09	1.23	1.08	0.99	0.99
1769100	1.09	1.08	1.12	1.03	1.03
1769200	1.09	1.27	1.05	1.04	1.04

historic data rescue and dissemination to develop improved hydrological models would be beneficial.

This research has evaluated the impact of explicit modelling of convective rainfall on river flow projections from lumped hydrological models for the first time, applied to a small number of catchments in the LVB and only using one lumped hydrological model, GR4J. Exploring the propagation of Δ95/Δmean through hydrological models of varying levels of complexity (lumped vs distributed, shorter timesteps) would be of benefit. This could include semi-distributed hydrological models (e.g. SWAT, which has been commonly used in East Africa (van Griensven et al., 2012)) as well as flood models (e.g. Miller et al. (2022)). Similarly,

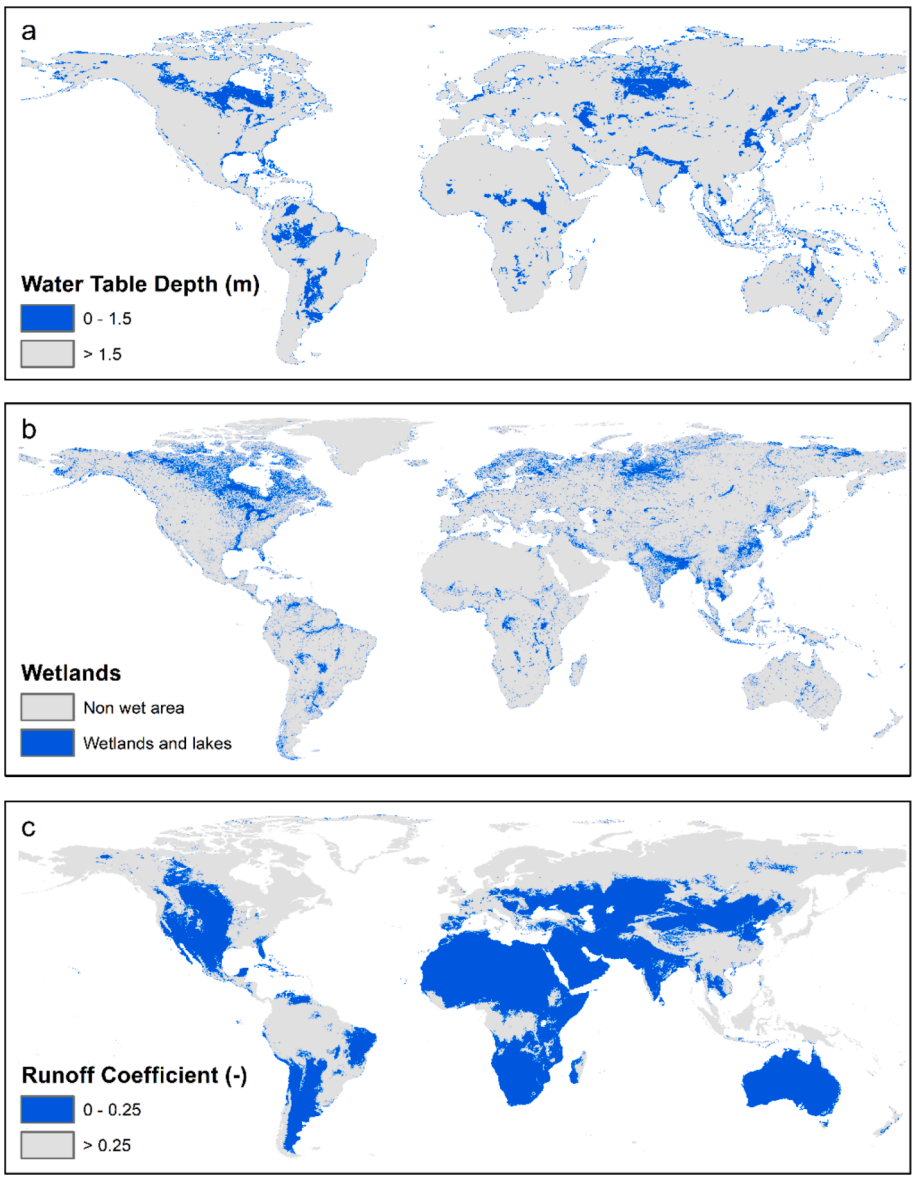

Fig. 7. Global maps of shallow water tables (panel a, modified after Fan et al. (2017)), wetlands (panel b, modified after Tootchi et al. (2019)) and runoff coefficient (panel c, modified after Beck et al. (2015)).

understanding propagation of Δ95/Δmean in catchments with varying hydrological attributes and projections of precipitation extremes would support an assessment of how useful CPM data are across different types of hydrological impact studies. This would require application of CPM data to hydrological models in areas where Δ95/Δmean for precipitation ≫ 1, as well as across catchments with varying degrees of baseflow contribution. Whilst CPMs improve the model performance for high intensity convective precipitation events, CPMs have also been shown to affect dry spell length in some African regions (Kendon et al., 2019). It would therefore be beneficial to undertake a complementary analysis with a focus on dry periods and low flow metrics.

In this study, only 10 years of weather data for the historic and future climate have been produced, and CP4 and R25 are simulations based on one GCM (the Met Office UM (Stratton et al., 2018)). The application of CP4 and R25 data to GR4J in this study also does not consider future land use change, which has been shown to have a potentially significant effect on water balance partitioning in the region (Gabiri et al., 2020; Näschen et al., 2019). The use of uncorrected climate model output as inputs to GR4J was intentional for this study for the purpose of evaluating the impact of explicit modelling of convective rainfall. However, in conjunction with the limitations above, the CP4 and R25 data cannot be used for climate change adaptation studies or planning at this time. Given that the character of precipitation time series (e.g. amplitude of extremes, duration of wet spells and dry spells) is important, any bias correction or downscaling of CPM data for such studies may need to consider the use of more sophisticated methods (quantile–quantile mapping, correction of dry day counts (e.g. Famien et al. (2018)), process based scaling of rainfall (e.g. Klein et al. (2021))) than simple approaches (e.g. delta change). Further work is required to assess how variability between convection permitting and non-convection permitting versions of the same GCM compares with variability between GCMs (e.g. within CMIP5 (Taylor et al., 2012)). Quantifying the balance of impacts of climate change on river flows from application of precipitation data from CPMs versus the impacts of future land use change would also be beneficial.

5. Conclusions

In this research we apply the outputs of a continental scale convection permitting (CP) climate model to five lumped rainfall-runoff models

in Africa for the first time. Application of a CP model produced greater river flows than an equivalent model using parameterised convection in both the current and future (c. 2100) climate in four of the five catchments. The location of the catchments near Lake Victoria resulted in unusually small changes in extreme rainfall relative to mean rainfall, likely explaining the small changes in extreme river flows relative to their mean change. The regional atmospheric physics causing this independence of future change on storm intensity requires further research.

Application of CP model rainfall data from an area where rainfall extremes change more than the change in mean rainfall to the rainfall-runoff model did not result in significant changes in river flows. This is shown to be a result of the rainfall-runoff model structure and parameterisation, which is likely to be due to large-scale storage in the catchments associated with wetland cover and groundwater storage, which buffers the impact of rainfall extremes. The hydrological conditions in which this buffering occurs are shown to be extensive across humid regions. Application of CP climate model data to lumped catchment models in these areas are unlikely to result in significant increases in extreme river flows relative to increases in mean flows.

Data availability statement

The GR4J model is available via the airGR package (Coron et al., 2017) in R (R Development Core Team, 2016). Daily river flow data in the Lake Victoria Basin are available from the Global Runoff Data Centre https://www.bafg.de/GRDC/EN/Home/homepage_node.html, GRDC, 56068 Koblenz, Germany) for non-commercial use only. Daily rainfall and temperature data from the WATCH forcing dataset (Weedon et al., 2011) are available at https://catalogue.ceh.ac.uk/documents/ba6e8ddd-22a9-457d-acf4-d63cd34f2dda. Mapping of the Lake Victoria Basin in Fig. 1 incorporates data from the HydroSHEDS version 1 database which is © World Wildlife Fund, Inc. (2006–2022) and has been used herein under license. WWF has not evaluated the data as altered and incorporated within this paper, and therefore gives no warranty regarding its accuracy, completeness, currency or suitability for any particular purpose. Portions of the HydroSHEDS v1 database incorporate data which are the intellectual property rights of © USGS (2006–2008), NASA (2000–2005), ESRI (1992–1998), CIAT (2004–2006), UNEP-WCMC (1993), WWF (2004), Commonwealth of Australia (2007), and Her Royal Majesty and the British Crown and are used under license. The HydroSHEDS v1 database and more information are available at https://www.hydrosheds.org. Data from the two climate model experiments ("CP4" and "R25", Stratton et al. (2018)) are available from https://catalogue.ceda.ac.uk/uuid/a6114f2319b34a58964dfa5305652fc6.

CRediT authorship contribution statement

M.J. Ascott: Conceptualization, Methodology, Formal analysis, Visualization, Writing – original draft. **V. Christelis:** Methodology, Software, Writing – review & editing. **D.J. Lapworth:** Conceptualization, Methodology, Writing – review & editing, Project administration, Supervision, Funding acquisition. **D.M..J. Macdonald:** Conceptualization, Methodology, Writing – review & editing, Supervision, Funding acquisition. **C. Tindimugaya:** Resources, Data curation, Supervision, Project administration. **A. Iragena:** Resources, Data curation, Project administration. **D. Finney:** Conceptualization, Methodology, Resources, Writing – review & editing. **R. Fitzpatrick:** Conceptualization, Methodology, Resources, Writing – review & editing. **J.H. Marsham:** Conceptualization, Methodology, Writing – review & editing, Project administration, Supervision, Funding acquisition. **D.P. Rowell:** Conceptualization, Methodology, Writing – review & editing, Supervision.

Declaration of Competing Interest

The authors declare that they have no known competing financial interests or personal relationships that could have appeared to influence the work reported in this paper.

Acknowledgements

MJA, VC, DJL and DMJM publish with permission of the Director, British Geological Survey. This research was undertaken primarily through funding provided by the UK Natural Environment Research Council (NERC) and the former Department for International Development (now Foreign, Commonwealth and Development Office) within the Future Climate for Africa Programme under the project HyCRISTAL (NE/M020452/1, NE/M019985/1, NE/M02038X/1). Additional support was provided by the British Geological Survey NC-ODA grant NE/R000069/1: Geoscience for Sustainable Futures and NERC MCNC Grant TerraFirma (NE/W004895/1).

Appendix A. Supplementary data

Supplementary data to this article can be found online at https://doi.org/10.1016/j.jhydrol.2023.129097.

References

Arsenault, R., Brissette, F., Martel, J.-L., 2018. The hazards of split-sample validation in hydrological model calibration. J. Hydrol. 566, 346–362. https://doi.org/10.1016/j.jhydrol.2018.09.027.

Ascott, M.J., Marchant, B.P., Macdonald, D., McKenzie, A.A., Bloomfield, J.P., 2017. Improved understanding of spatio-temporal controls on regional scale groundwater flooding using hydrograph analysis and impulse response functions. Hydrol. Processes 31 (25), 4586–4599. https://doi.org/10.1002/hyp.11380.

Atawneh, D.A., Cartwright, N., Bertone, E., 2021. Climate change and its impact on the projected values of groundwater recharge: a review. J. Hydrol. 601, 126602 https://doi.org/10.1016/j.jhydrol.2021.126602.

Ayugi, B., Zhihong, J., Zhu, H., Ngoma, H., Babaousmail, H., Rizwan, K., Dike, V., 2021. Comparison of CMIP6 and CMIP5 models in simulating mean and extreme precipitation over East Africa. Int. J. Climatol. 41 (15), 6474–6496. https://doi.org/10.1002/joc.7207.

Beck, H.E., de Roo, A., van Dijk, A.I.J.M., 2015. Global maps of streamflow characteristics based on observations from several thousand catchments. J. Hydrometeorol. 16 (4), 1478–1501. https://doi.org/10.1175/jhm-d-14-0155.1.

Bergström, S., 1995. The HBV model. Computer models of watershed hydrology. 443-476.

Berthou, S., Kendon, E.J., Chan, S.C., Ban, N., Leutwyler, D., Schär, C., Fosser, G., 2020. Pan-European climate at convection-permitting scale: a model intercomparison study. Clim. Dyn. 55 (1), 35–59. https://doi.org/10.1007/s00382-018-4114-6.

Bock, O., Guichard, F., Meynadier, R., Gervois, S., Agustí-Panareda, A., Beljaars, A., Boone, A., Nuret, M., Redelsperger, J.-L., Roucou, P., 2011. The large-scale water cycle of the West African monsoon. Atmos. Sci. Lett. 12 (1), 51–57. https://doi.org/10.1002/asl.288.

Bodian, A., Dezetter, A., Diop, L., Deme, A., Djaman, K., Diop, A., 2018. Future climate change impacts on streamflows of two main West Africa river basins: Senegal and Gambia. Hydrology 5 (1), 21.

Bornemann, F.J., Rowell, D.P., Evans, B., Lapworth, D.J., Lwiza, K., Macdonald, D.M.J., Marsham, J.H., Tesfaye, K., Ascott, M.J., Way, C., 2019. Future changes and uncertainty in decision-relevant measures of East African climate. Clim. Change 156 (3), 365–384.

Christensen, J.H., Christensen, O.B., 2003. Climate modelling: severe summertime flooding in Europe. Nature 421 (6925), 805–806.

Clark, P., Roberts, N., Lean, H., Ballard, S.P., Charlton-Perez, C., 2016. Convection-permitting models: a step-change in rainfall forecasting. Meteorol. Appl. 23 (2), 165–181. https://doi.org/10.1002/met.1538.

Conover, W.J., 1999. Practical Nonparametric Statistics, 350. John Wiley & Sons.

Coron, L., Thirel, G., Delaigue, O., Perrin, C., Andréassian, V., 2017. The suite of lumped GR hydrological models in an R package. Environ. Model. Softw. 94, 166–171. https://doi.org/10.1016/j.envsoft.2017.05.002.

Cuthbert, M.O., Taylor, R.G., Favreau, G., Todd, M.C., Shamsudduha, M., Villholth, K.G., MacDonald, A.M., Scanlon, B.R., Kotchoni, D.O.V., Vouillamoz, J.-M., Lawson, F.M.A., Adjomayi, P.A., Kashaigili, J., Seddon, D., Sorensen, J.P.R., Ebrahim, G.Y., Owor, M., Nyenje, P.M., Nazoumou, Y., Goni, I., Ousmane, B.I., Sibanda, T., Ascott, M.J., Macdonald, D.M.J., Agyekum, W., Koussoubé, Y., Wanke, H., Kim, H., Wada, Y., Lo, M.-H., Oki, T., Kukuric, N., 2019. Observed controls on resilience of groundwater to climate variability in sub-Saharan Africa. Nature 572 (7768), 230–234. https://doi.org/10.1038/s41586-019-1441-7.

Dessu, S.B., Melesse, A.M., 2013. Impact and uncertainties of climate change on the hydrology of the Mara River basin, Kenya/Tanzania. Hydrol. Processes 27 (20), 2973–2986. https://doi.org/10.1002/hyp.9434.
DHI, 2008. MIKE SHE User Guide., DHI, Water and Environment, Hørsholm, Denmark.
Dirmeyer, P.A., Cash, B.A., Kinter, J.L., Jung, T., Marx, L., Satoh, M., Stan, C., Tomita, H., Towers, P., Wedi, N., Achuthavarier, D., Adams, J.M., Altshuler, E.L., Huang, B., Jin, E.K., Manganello, J., 2012. Simulating the diurnal cycle of rainfall in global climate models: resolution versus parameterization. Clim. Dyn. 39 (1), 399–418. https://doi.org/10.1007/s00382-011-1127-9.
Dunning, C.M., Black, E., Allan, R.P., 2018. Later wet seasons with more intense rainfall over Africa under future climate change. J. Clim. 31 (23), 9719–9738. https://doi.org/10.1175/JCLI-D-18-0102.1.
Famien, A.M., Janicot, S., Ochou, A.D., Vrac, M., Defrance, D., Sultan, B., Noël, T., 2018. A bias-corrected CMIP5 dataset for Africa using the CDF-t method – a contribution to agricultural impact studies. Earth Syst. Dynam. 9 (1), 313–338. https://doi.org/10.5194/esd-9-313-2018.
Fan, Y., Miguez-Macho, G., Jobbágy, E.G., Jackson, R.B., Otero-Casal, C., 2017. Hydrologic regulation of plant rooting depth. Proc. Natl. Acad. Sci. 114 (40), 10572–10577. https://doi.org/10.1073/pnas.1712381114.
Finney, D.L., Marsham, J.H., Jackson, L.S., Kendon, E.J., Rowell, D.P., Boorman, P.M., Keane, R.J., Stratton, R.A., Senior, C.A., 2019. Implications of improved representation of convection for the East Africa water budget using a convection-permitting model. J. Clim. 32 (7), 2109–2129. https://doi.org/10.1175/jcli-d-18-0387.1.
Finney, D.L., Marsham, J.H., Rowell, D.P., Kendon, E.J., Tucker, S.O., Stratton, R.A., Jackson, L.S., 2020. Effects of explicit convection on future projections of mesoscale circulations, rainfall, and rainfall extremes over Eastern Africa. J. Clim. 33 (7), 2701–2718. https://doi.org/10.1175/jcli-d-19-0328.1.
Fowler, H.J., Blenkinsop, S., Tebaldi, C., 2007. Linking climate change modelling to impacts studies: recent advances in downscaling techniques for hydrological modelling. Int. J. Climatol. 27 (12), 1547–1578. https://doi.org/10.1002/joc.1556.
Gabiri, G., Diekkrüger, B., Näschen, K., Leemhuis, C., van der Linden, R., Majaliwa, J.-G.-M., Obando, J.A., 2020. Impact of climate and land use/land cover change on the water resources of a tropical inland valley catchment in Uganda, East Africa. Climate 8 (7), 83.
Garrote, L., 2017. Managing water resources to adapt to climate change: facing uncertainty and scarcity in a changing context. Water Resour. Manag. 31 (10), 2951–2963. https://doi.org/10.1007/s11269-017-1714-6.
Githui, F., Gitau, W., Mutua, F., Bauwens, W., 2009. Climate change impact on SWAT simulated streamflow in western Kenya. Int. J. Climatol. 29 (12), 1823–1834. https://doi.org/10.1002/joc.1828.
Golding, B., Roberts, N., Leoncini, G., Mylne, K., Swinbank, R., 2016. MOGREPS-UK convection-permitting ensemble products for surface water flood forecasting: rationale and first results. J. Hydrometeorol. 17 (5), 1383–1406. https://doi.org/10.1175/jhm-d-15-0083.1.
GRDC, 2011. Watershed Boundaries of GRDC Stations / Global Runoff Data Centre. In: (BfG), F.I.o.H. (Ed.), Koblenz, Germany.
Gupta, H.V., Kling, H., Yilmaz, K.K., Martinez, G.F., 2009. Decomposition of the mean squared error and NSE performance criteria: Implications for improving hydrological modelling. J. Hydrol. 377 (1–2), 80–91.
Gyawali, R., Watkins, D.W., 2013. Continuous hydrologic modeling of snow-affected watersheds in the great lakes basin using HEC-HMS. J. Hydrol. Eng. 18 (1), 29–39. https://doi.org/10.1061/(ASCE)HE.1943-5584.0000591.
Hanley, K.E., Pirret, J.S.R., Bain, C.L., Hartley, A.J., Lean, H.W., Webster, S., Woodhams, B.J., 2021. Assessment of convection-permitting versions of the Unified Model over the Lake Victoria basin region. Q. J. R. Meteorolog. Soc. 147 (736), 1642–1660. https://doi.org/10.1002/qj.3988.
Jackson, L.S., Finney, D.L., Kendon, E.J., Marsham, J.H., Parker, D.J., Stratton, R.A., Tomassini, L., Tucker, S., 2020. The effect of explicit convection on couplings between rainfall, humidity, and ascent over Africa under climate change. J. Clim. 33 (19), 8315–8337. https://doi.org/10.1175/jcli-d-19-0322.1.
Kay, A., 2022. Differences in hydrological impacts using regional climate model and nested convection-permitting model data. Clim. Change 173 (1), 11. https://doi.org/10.1007/s10584-022-03405-z.
Kay, A.L., Davies, H.N., 2008. Calculating potential evaporation from climate model data: a source of uncertainty for hydrological climate change impacts. J. Hydrol. 358 (3–4), 221–239. https://doi.org/10.1016/j.jhydrol.2008.06.005.
Kendon, E.J., Ban, N., Roberts, N.M., Fowler, H.J., Roberts, M.J., Chan, S.C., Evans, J.P., Fosser, G., Wilkinson, J.M., 2017. Do convection-permitting regional climate models improve projections of future precipitation change? Bull. Am. Meteorol. Soc. 98 (1), 79–93.
Kendon, E.J., Stratton, R.A., Tucker, S., Marsham, J.H., Berthou, S., Rowell, D.P., Senior, C.A., 2019. Enhanced future changes in wet and dry extremes over Africa at convection-permitting scale. Nat. Commun. 10 (1), 1794. https://doi.org/10.1038/s41467-019-09776-9.
Kendon, E.J., Prein, A.F., Senior, C.A., Stirling, A., 2021. Challenges and outlook for convection-permitting climate modelling. Philos. Trans. R. Soc. A Math. Phys. Eng. Sci. 379 (2195), 20190547. https://doi.org/10.1098/rsta.2019.0547.
Kingston, D.G., Taylor, R.G., 2010. Sources of uncertainty in climate change impacts on river discharge and groundwater in a headwater catchment of the Upper Nile Basin, Uganda. Hydrol. Earth Syst. Sci. 14 (7), 1297–1308. https://doi.org/10.5194/hess-14-1297-2010.
Klein, C., Jackson, L.S., Parker, D.J., Marsham, J.H., Taylor, C.M., Rowell, D.P., Guichard, F., Vischel, T., Famien, A.M., Diedhiou, A., 2021. Combining CMIP data with a regional convection-permitting model and observations to project extreme rainfall under climate change. Environ. Res. Lett. 16 (10), 104023 https://doi.org/10.1088/1748-9326/ac26f1.
Knoben, W.J.M., Freer, J.E., Woods, R.A., 2019. Technical note: Inherent benchmark or not? Comparing Nash-Sutcliffe and Kling-Gupta efficiency scores. Hydrol. Earth Syst. Sci. 23 (10), 4323–4331. https://doi.org/10.5194/hess-23-4323-2019.
Kodja, D.J., Akognongbé, A.J.S., Amoussou, E., Mahé, G., Vissin, E.W., Paturel, J.E., Houndénou, C., 2020. Calibration of the hydrological model GR4J from potential evapotranspiration estimates by the Penman-Monteith and Oudin methods in the Ouémé watershed (West Africa). Proc. IAHS 383, 163–169. https://doi.org/10.5194/piahs-383-163-2020.
Kusangaya, S., Warburton, M.L., Archer van Garderen, E., Jewitt, G.P.W., 2014. Impacts of climate change on water resources in southern Africa: a review. Phys. Chem. Earth, Parts A/B/C 67–69, 47–54. https://doi.org/10.1016/j.pce.2013.09.014.
Le Lay, M., Galle, S., Saulnier, G.M., Braud, I., 2007. Exploring the relationship between hydroclimatic stationarity and rainfall-runoff model parameter stability: a case study in West Africa. Water Resour. Res. 43 (7) https://doi.org/10.1029/2006WR005257.
Lehner, B., Grill, G., 2013. Global river hydrography and network routing: baseline data and new approaches to study the world's large river systems. Hydrol. Processes 27 (15), 2171–2186. https://doi.org/10.1002/hyp.9740.
Lehner, B., Verdin, K., Jarvis, A., 2008. New global hydrography derived from spaceborne elevation data. Eos Trans. AGU 89 (10), 93–94.
Linke, S., Lehner, B., Ouellet Dallaire, C., Ariwi, J., Grill, G., Anand, M., Beames, P., Burchard-Levine, V., Maxwell, S., Moidu, H., Tan, F., Thieme, M., 2019. Global hydro-environmental sub-basin and river reach characteristics at high spatial resolution. Sci. Data 6 (1), 283. https://doi.org/10.1038/s41597-019-0300-6.
Liu, C., Ikeda, K., Rasmussen, R., Barlage, M., Newman, A.J., Prein, A.F., Chen, F., Chen, L., Clark, M., Dai, A., Dudhia, J., Eidhammer, T., Gochis, D., Gutmann, E., Kurkute, S., Li, Y., Thompson, G., Yates, D., 2017. Continental-scale convection-permitting modeling of the current and future climate of North America. Clim. Dyn. 49 (1), 71–95. https://doi.org/10.1007/s00382-016-3327-9.
Mehdi, B., Dekens, J., Herrnegger, M., 2021. Climatic impacts on water resources in a tropical catchment in Uganda and adaptation measures proposed by resident stakeholders. Clim. Change 164 (1), 10. https://doi.org/10.1007/s10584-021-02958-9.
Meresa, H.K., Gatachew, M.T., 2018. Climate change impact on river flow extremes in the Upper Blue Nile River basin. J. Water Clim. Change 10 (4), 759–781. https://doi.org/10.2166/wcc.2018.154.
Miller, J.D., Vischel, T., Fowe, T., Panthou, G., Wilcox, C., Taylor, C.M., Visman, E., Coulibaly, G., Gonzalez, P., Body, R., Vesuviano, G., Bouvier, C., Chahinian, N., Cazenave, F., 2022. A modelling-chain linking climate science and decision-makers for future urban flood management in West Africa. Reg. Environ. Chang. 22 (3), 93. https://doi.org/10.1007/s10113-022-01943-x.
Näschen, K., Diekkrüger, B., Evers, M., Höllermann, B., Steinbach, S., Thonfeld, F., 2019. The impact of land use/land cover change (LULCC) on water resources in a tropical catchment in Tanzania under different climate change scenarios. Sustainability 11 (24), 7083.
Ngoran, S.D., Dogah, K.E., Xue, X., 2015. Assessing the impacts of climate change on water resources: the Sub-Saharan Africa perspective. J. Econ. Sustain. Dev. 6 (1), 185–193.
Perrin, C., Michel, C., Andréassian, V., 2003. Improvement of a parsimonious model for streamflow simulation. J. Hydrol. 279 (1), 275–289. https://doi.org/10.1016/S0022-1694(03)00225-7.
Pirazzoli, P.A., Costa, S., Dornbusch, U., Tomasin, A., 2006. Recent evolution of surge-related events and assessment of coastal flooding risk on the eastern coasts of the English Channel. Ocean Dyn. 56 (5), 498–512. https://doi.org/10.1007/s10236-005-0040-3.
Qing, Y., Wang, S., Zhang, B., Wang, Y., 2020. Ultra-high resolution regional climate projections for assessing changes in hydrological extremes and underlying uncertainties. Clim. Dyn. 55 (7), 2031–2051. https://doi.org/10.1007/s00382-020-05372-6.
R Development Core Team, 2016. R: A Language and Environment for Statistical Computing. R Foundation for Statistical Computing, Vienna, Austria.
Reszler, C., Switanek, M.B., Truhetz, H., 2018. Convection-permitting regional climate simulations for representing floods in small- and medium-sized catchments in the Eastern Alps. Nat. Hazards Earth Syst. Sci. 18 (10), 2653–2674. https://doi.org/10.5194/nhess-18-2653-2018.
Roca, R., Aublanc, J., Chambon, P., Fiolleau, T., Viltard, N., 2014. Robust observational quantification of the contribution of mesoscale convective systems to rainfall in the Tropics. J. Clim. 27 (13), 4952–4958. https://doi.org/10.1175/jcli-d-13-00628.1.
Rowell, D.P., Berthou, S., 2022. Fine-scale climate projections: what additional fixed spatial detail is provided by a convection-permitting model? J. Clim. 1–36 https://doi.org/10.1175/jcli-d-22-0009.1.
Schaller, N., Sillmann, J., Müller, M., Haarsma, R., Hazeleger, W., Hegdahl, T.J., Kelder, T., van den Oord, G., Weerts, A., Whan, K., 2020. The role of spatial and temporal model resolution in a flood event storyline approach in western Norway. Weather Clim. Extremes 29, 100259. https://doi.org/10.1016/j.wace.2020.100259.
Senior, C.A., Marsham, J.H., Berthou, S., Burgin, L.E., Folwell, S.S., Kendon, E.J., Klein, C.M., Jones, R.G., Mittal, N., Rowell, D.P., Tomassini, L., Vischel, T., Becker, B., Birch, C.E., Crook, J., Dougill, A.J., Finney, D.L., Graham, R.J., Hart, N.C.G., Jack, C.D., Jackson, L.S., James, R., Koelle, B., Misiani, H., Mwalukanga, B., Parker, D.J., Stratton, R.A., Taylor, C.M., Tucker, S.O., Wainwright, C.M., Washington, R., Willet, M.R., 2021. Convection-permitting regional climate change simulations for understanding future climate and informing decision-making in Africa. Bull. Am. Meteorol. Soc. 102 (6), E1206–E1223. https://doi.org/10.1175/bams-d-20-0020.1.

Siam, M.S., Eltahir, E.A.B., 2017. Climate change enhances interannual variability of the Nile river flow. Nat. Clim. Chang. 7 (5), 350–354. https://doi.org/10.1038/nclimate3273.

Stephens, G.L., L'Ecuyer, T., Forbes, R., Gettelmen, A., Golaz, J.-C., Bodas-Salcedo, A., Suzuki, K., Gabriel, P., Haynes, J., 2010. Dreary state of precipitation in global models. J. Geophys. Res. Atmos. 115 (D24) https://doi.org/10.1029/2010JD014532.

Stratton, R.A., Senior, C.A., Vosper, S.B., Folwell, S.S., Boutle, I.A., Earnshaw, P.D., Kendon, E., Lock, A.P., Malcolm, A., Manners, J., Morcrette, C.J., Short, C., Stirling, A.J., Taylor, C.M., Tucker, S., Webster, S., Wilkinson, J.M., 2018. A Pan-African convection-permitting regional climate simulation with the met office unified model: CP4-Africa. J. Clim. 31 (9), 3485–3508. https://doi.org/10.1175/jcli-d-17-0503.1.

Taye, M.T., Ntegeka, V., Ogiramoi, N.P., Willems, P., 2011. Assessment of climate change impact on hydrological extremes in two source regions of the Nile River Basin. Hydrol. Earth Syst. Sci. 15 (1), 209–222. https://doi.org/10.5194/hess-15-209-2011.

Taylor, K.E., Stouffer, R.J., Meehl, G.A., 2012. An overview of CMIP5 and the experiment design. Bull. Am. Meteorol. Soc. 93 (4), 485–498. https://doi.org/10.1175/bams-d-11-00094.1.

Taylor, R.G., Todd, M.C., Kongola, L., Maurice, L., Nahozya, E., Sanga, H., MacDonald, A. M., 2013. Evidence of the dependence of groundwater resources on extreme rainfall in East Africa. Nat. Clim. Chang. 3 (4), 374–378. https://doi.org/10.1038/nclimate1731.

Thornthwaite, C.W., 1948. An approach toward a rational classification of climate. Geogr. Rev. 38 (1), 55–94. https://doi.org/10.2307/210739.

Tootchi, A., Jost, A., Ducharne, A., 2019. Multi-source global wetland maps combining surface water imagery and groundwater constraints. Earth Syst. Sci. Data 11 (1), 189–220. https://doi.org/10.5194/essd-11-189-2019.

Tramblay, Y., Rouché, N., Paturel, J.E., Mahé, G., Boyer, J.F., Amoussou, E., Bodian, A., Dacosta, H., Dakhlaoui, H., Dezetter, A., Hughes, D., Hanich, L., Peugeot, C., Tshimanga, R., Lachassagne, P., 2021. ADHI: the African database of hydrometric indices (1950–2018). Earth Syst. Sci. Data 13 (4), 1547–1560. https://doi.org/10.5194/essd-13-1547-2021.

Van de Walle, J., Thiery, W., Brousse, O., Souverijns, N., Demuzere, M., van Lipzig, N.P. M., 2020. A convection-permitting model for the Lake Victoria Basin: evaluation and insight into the mesoscale versus synoptic atmospheric dynamics. Clim. Dyn. 54 (3), 1779–1799. https://doi.org/10.1007/s00382-019-05088-2.

van Griensven, A., Ndomba, P., Yalew, S., Kilonzo, F., 2012. Critical review of SWAT applications in the upper Nile basin countries. Hydrol. Earth Syst. Sci. 16 (9), 3371–3381. https://doi.org/10.5194/hess-16-3371-2012.

Vincendon, B., Ducrocq, V., Nuissier, O., Vié, B., 2011. Perturbation of convection-permitting NWP forecasts for flash-flood ensemble forecasting. Nat. Hazards Earth Syst. Sci. 11 (5), 1529–1544. https://doi.org/10.5194/nhess-11-1529-2011.

Wainwright, C.M., Finney, D.L., Kilavi, M., Black, E., Marsham, J.H., 2021a. Extreme rainfall in East Africa, October 2019–January 2020 and context under future climate change. Weather 76 (1), 26–31. https://doi.org/10.1002/wea.3824.

Wainwright, C.M., Marsham, J.H., Rowell, D.P., Finney, D.L., Black, E., 2021b. Future changes in seasonality in East Africa from regional simulations with explicit and parameterized convection. J. Clim. 34 (4), 1367–1385. https://doi.org/10.1175/jcli-d-20-0450.1.

Wang, S., Wang, Y., 2019. Improving probabilistic hydroclimatic projections through high-resolution convection-permitting climate modeling and Markov chain Monte Carlo simulations. Clim. Dyn. 53 (3), 1613–1636. https://doi.org/10.1007/s00382-019-04702-7.

Webster, R., Oliver, M.A., 1990. Statistical Methods in Soil and Land Resource Survey. Oxford University Press (OUP).

Weedon, G.P., Gomes, S., Viterbo, P., Shuttleworth, W.J., Blyth, E., Österle, H., Adam, J. C., Bellouin, N., Boucher, O., Best, M., 2011. Creation of the WATCH forcing data and its use to assess global and regional reference crop evaporation over land during the twentieth century. J. Hydrometeorol. 12 (5), 823–848. https://doi.org/10.1175/2011jhm1369.1.

Westra, S., Thyer, M., Leonard, M., Kavetski, D., Lambert, M., 2014. A strategy for diagnosing and interpreting hydrological model nonstationarity. Water Resour. Res. 50 (6), 5090–5113. https://doi.org/10.1002/2013WR014719.

Wilby, R.L., Dawson, C.W., Yu, D., Herring, Z., Baruch, A., Ascott, M.J., Finney, D.L., Macdonald, D.M.J., Marsham, J.H., Matthews, T., Murphy, C., 2022. Spatial and temporal scaling of sub-daily extreme rainfall for data sparse places. Clim. Dyn. https://doi.org/10.1007/s00382-022-06528-2.

Wu, H., Adler, R.F., Hong, Y., Tian, Y., Policelli, F., 2012. Evaluation of global flood detection using satellite-based rainfall and a hydrologic model. J. Hydrometeorol. 13 (4), 1268–1284.

Yu, D., Lane, S.N., 2006. Urban fluvial flood modelling using a two-dimensional diffusion-wave treatment, part 1: mesh resolution effects. Hydrol. Processes 20 (7), 1541–1565. https://doi.org/10.1002/hyp.5935.

Zhang, B., Wang, S., Wang, Y., 2021. Probabilistic projections of multidimensional flood risks at a convection-permitting scale. e2020WR028582 Water Resour. Res. 57 (1). https://doi.org/10.1029/2020WR028582.